A Back-emf Based Method to Detect Magnet Failures in PMSMs

Julio-César URRESTY (First author)
julio.urresty@mcia.upc.edu
Electronic Engineering Dept., Universitat Politècnica de Catalunya
Edifici Gaia, Rambla Sant Nebridi, 08222 Terrassa, Barcelona, Spain
Tel. +34 937398560

Second author + Corresponding Author:
Jordi-Roger RIBA, member IEEE
jordi@euetii.upc.edu
Escola d'Enginyeria d'Igualada
Electrical Engineering Dept., Universitat Politècnica de Catalunya
Plaça del Rei 15, 08700 Igualada, Barcelona, Spain
Tel.: +34 938035300
Fax.: +34 938031589

Third author:
Luís ROMERAL, member IEEE
romeral@eel.upc.edu
Electronic Engineering Dept., Universitat Politècnica de Catalunya, SPAIN
Edifici Gaia, Rambla Sant Nebridi, 08222 Terrassa, Barcelona, Spain
Tel. +34 937398510

Abstract – **Demagnetization faults are troublesome because they have a profound impact on the overall performance of permanent magnet synchronous motors (PMSMs). This work presents and verifies experimentally a system to detect such faults which is based on the measure of the zero sequence voltage component (ZSVC). The proposed method is also appropriate for inverter fed machines and is particularly useful when dealing with fault tolerant systems. A fault severity index which allows quantifying the harshness of such faults is also proposed and its behavior is analyzed from experimental data. Features of the proposed method include low computational burden, simplicity and high sensitivity. Experimental results conducted at different speed and load conditions show the potential of the proposed fault severity index for online diagnosis of demagnetization failures.**

Index Terms –**Fault diagnosis, permanent magnet synchronous machines, demagnetization, zero sequence voltage component.**

I. INTRODUCTION

Nowadays, permanent magnet synchronous (PMSM) are a serious option for electric traction systems. Electric vehicle motors require compactness, broad speed and torque range and high efficiency. Particularly, PMSMs are well-positioned candidates for hybrid and electric vehicle power train with compact structure [1]. This is because they offer highly attractive features, including high efficiency, precise torque control, high power density and high torque to current ratio among others [2,3].

In high performance applications, the rotor magnets are usually made of sintered rare earth materials such as NdFeB. Such materials are easy to crack, brittle and easy to erode owing to high humidity or dew. During installation the permanent magnets are exposed to mechanical pressure which may cause small cracks which may lead to disintegration at high speed [4]. A direct impact on the motor may also damage the magnets, leading to partial demagnetization [5]. Additionally, under certain circumstances, the magnets may be exposed to different types of contaminants, including dust pollution, salt and cooling lubricants among others, which also may lead to disintegration.

Demagnetization is one of the failure causes of most concern in these types of machines. Partial demagnetization has adverse mechanical effects because it causes unbalanced magnetic pull, magnetic force harmonics, acoustic noise and vibrations [6], thus reducing considerably the mechanical torque of the PMSM and severely affecting motor performance [7].

The stator currents generate a reverse magnetic field which is opposed to the remanent induction of the rotor magnets. This effect is particularly important when strong torque is required. This reiterated phenomenon may lead to partial

demagnetization in the permanent magnets [2]. Due to partial demagnetization, the PMSM requires a stator current higher than the rated one to generate the same output torque. This in turn increases the temperature of the PMSM and may cause more demagnetization, which again increases the stator current [8]. Additionally, over currents due to inter-turn short circuits may produce partial demagnetization [7]. The worst-case condition happens when a whole stator coil is in short circuit when the armature reaction is at its highest, during transients or when the motor drives high loads [6]. Stator short circuits help increase the fault effects and may shift the permanent magnet operating point below the irreversible demagnetization region [1].

This study deals with surface-mounted permanent magnet synchronous motors (SPMSMs) with symmetrical concentrated stator windings connected in series. Although this work is devoted to surface-mounted PMSMs, the results obtained may be extrapolated to other PMSM geometries. In this work it is proved that in this type of motor, partial demagnetization faults generate harmonics in the spectrum of the back-emf of a single slot because the flux linking the stator windings is not symmetrical. However, depending on the windings configuration, when analyzing the global back-emf induced in all the slots of a phase, in some cases it is not possible to detect such harmonics because they cancel each other. Hence, when diagnosing this specific type of fault in the kind of motor under study, it is not feasible to detect fault harmonics in the current spectrum due to demagnetization.

In [9] it is proposed to study the torque constant as a fault indicator for diagnosing demagnetization faults when dealing with trapezoidal flux brushless DC motors. This fault indicator is obtained from an estimation of the back-emf. However, the torque constant calculated by this method has inherent estimation errors. In case of low demagnetization degrees or low speed operation, this error may mask the small changes in the back-emf with respect to the healthy condition. Hence, a direct reading may overcome this drawback.

Consequently, in this work it is proposed to diagnose incipient demagnetization faults by applying an online monitoring of the zero-sequence voltage component (ZSVC). This method is also appropriate for inverter-fed machines. An accessible neutral point of the stator windings is needed to measure the ZSVC, just as required by the fault tolerant schemes that add an extra inverter branch which, under a fault condition, is connected to the neutral point of the SPMSM by replacing the faulty phase [10-11]. Additionally, a simple-to-extract fault severity factor is presented and its behavior is evaluated and validated by means of experiments when the SPMSM operates under different speed and load conditions.

II. THE SPMSM ANALYZED

In this section the effects of partial demagnetization faults are analyzed by means of FEM simulations and experimental results. The analyzed SPMSM has symmetrical concentrated stator windings connected in series and the rotor has skewing. This effect has been taken into consideration as explained hereafter. Additional parameters of the analyzed SPMSM are given in Table I. They are used to generate the FEM model whose simulation results are presented in the following sections.

TABLE I
GEOMETRIC PARAMETERS AND MATERIALS OF THE SPMSMS ANALYZED.

Manufacturer	ABB
Converter model	DGV 700
Rated voltage	380 Vac
Rated current	2.9 A
Rated torque	2.3 Nm
Rated speed	6000 r/min
Poles pairs	3
Stator slots	18
Stator slots per phase	6
N	144 turns/phase
R_s	1.50 Ω (1.1% unbalance)
L	4.9 mH
M	-0.89 mH
Magnets type	NdFeB
Magnets per pole	4
Magnets remanent magnetic flux density	1.18 T
Stator steel saturation magnetic flux density	1.8 T
Axial length	89 mm
Stator outer radius	40.49 mm
Air gap	0.6 mm
Rotor outer radius	22.8 mm
Magnets height	2.5 mm
Shaft radius	9 mm

It is supposed that the faulty SPMSM has two poles 50% partially demagnetized as shown in Figs. 1 and 2.

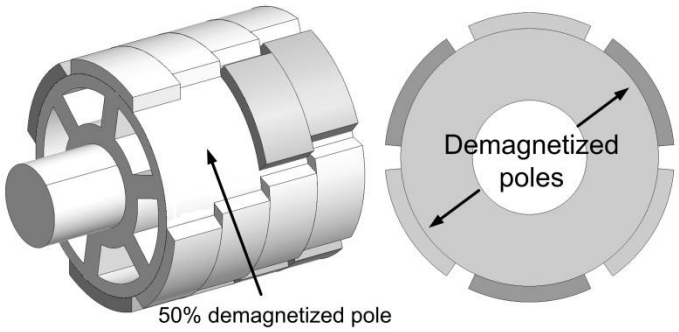

Fig. 1. Type of demagnetization analyzed in this work.

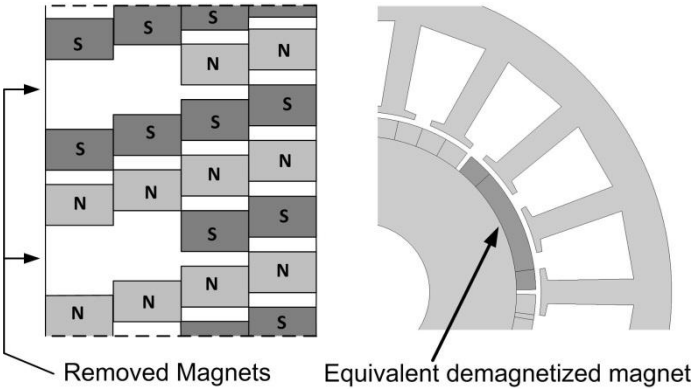

Fig. 2. Equivalent rotor magnets distribution and geometry used in FEM simulations.

Fig. 3 shows the magnetic flux density distribution generated by the partially demagnetized rotor. It deals with the rotor skewed geometry and assumes two out of the four magnets have been removed. Detailed information about the method to take into account the rotor skew effect may be found in [12].

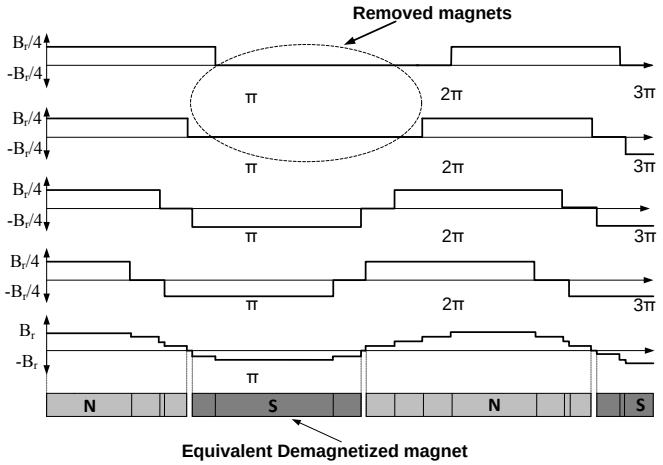

Fig. 3. Distribution of the magnetic flux density for the partially demagnetized skewed rotor analyzed and resulting magnets geometry applied in FEM simulations.

Experiments were carried out by means of healthy and faulty SPMSMs according to the scheme presented in Fig. 4. It shows an ABB 380 Vac motor driven by an ABB DGV 700 power converter. The motor was loaded with an identical SPMSM that acted as a load, driven by a torque controller. The $V_{0,m}$ ZSVC was measured by means of a LEM AV 100-50 voltage transducer with nominal voltage 50 Vrms and the stator currents were acquired by means of three Tektronix A622 ac/dc current probes. Data acquisition was carried out by using a data acquisition board NI PCI-6251 with 16 input channels, as detailed in Fig. 4.

The SPMSM acting as a motor was modified according to Fig. 1. The neutral point of its stator windings was made accessible as well as the two terminals of a pair of poles of phase *a* winding (coil a_1-$a_{1'}$ in Fig. 5). Additionally, the four removed rotor magnets were placed in opposite positions in order to balance the magnetic forces on the rotor, thus avoiding mechanical effects. Afterwards the rotor mass was balanced.

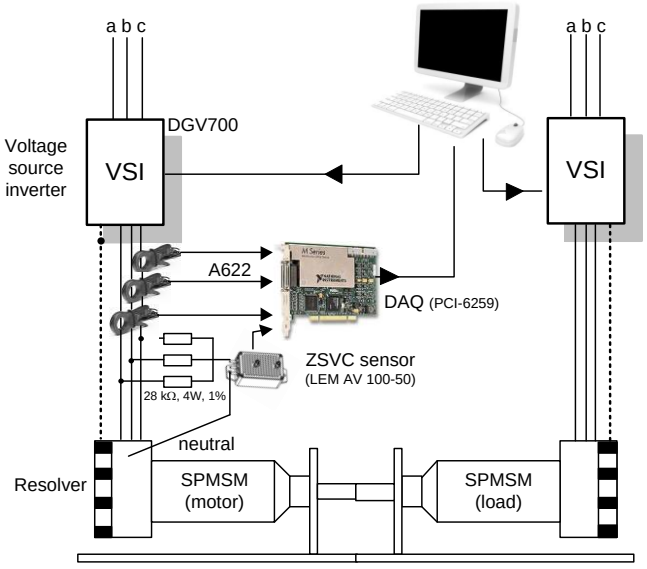

Fig. 4. Experimental rig.

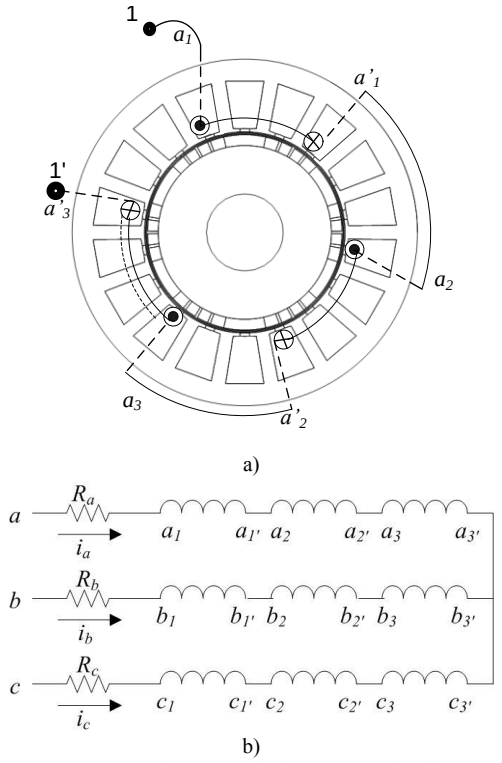

Fig. 5. a) SPMSM geometry. b) Stator windings connection diagram.

In the technical literature [2,13] it is reported that partial demagnetization leads to harmonic frequencies in the stator currents according to,

$$f_{demag} = f_e\left(1 \pm \frac{h}{p}\right) \quad h = 1,2,3,... \tag{1}$$

where f_{demag} are the fault harmonic frequencies, while f_e is the supply frequency and p is the number of pole pairs. Note that according to (1), the stator currents spectrum may contain fractional as well as odd harmonics of the electrical frequency. However, in this section it is shown that by using the specific

stator windings configuration shown in Fig. 5, the fault harmonics predicted by (1) are not present in the current spectrum.

Fig. 6 shows the back-emf induced in a pair of slots –a single pole of a phase winding– when the machine operates as a generator. It can be clearly appreciated that every time the removed magnets pass in front of the studied pole of the phase winding, the back-emf voltage is reduced.

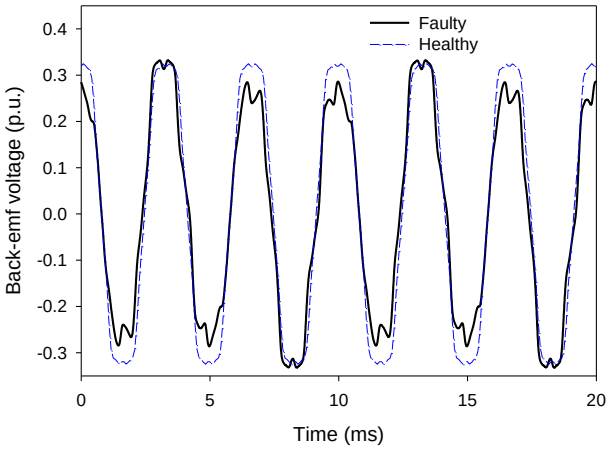

a)

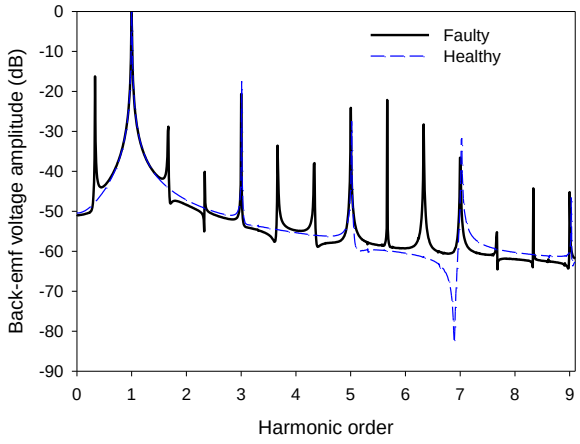

b)

Fig. 6. FEM simulations of a healthy and a faulty SPMSM operating as a generator. a) Normalized back-emf –with respect to the phase voltage– induced in a pole of a phase winding (two slots) when operating at 6000 r/min. b) Back-emf voltage spectrum.

Results from Fig. 6b are in close agreement with (1) since the back-emf spectrum induced in a single pole of a phase winding contains odd and fractional harmonics of the supply frequency.

To validate the usefulness of the FEM simulations shown in Fig. 6a, an experimental acquisition of the back-emf voltage induced in a pair of slots is presented in Fig 7a. It shows a close similarity with the simulation results. Additionally, the experimental back-emf spectrum of Fig. 7b clearly shows the presence of fractional harmonics similar to that in Fig. 6b.

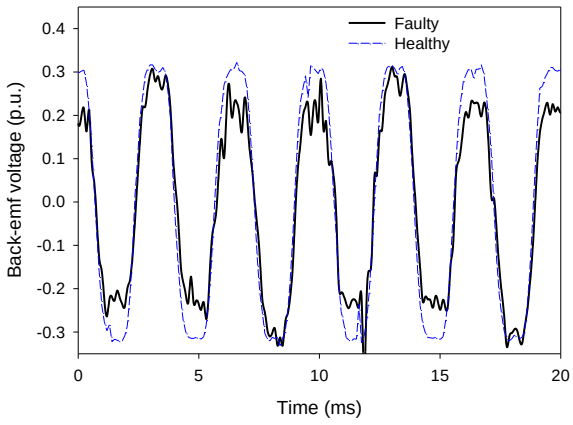

a)

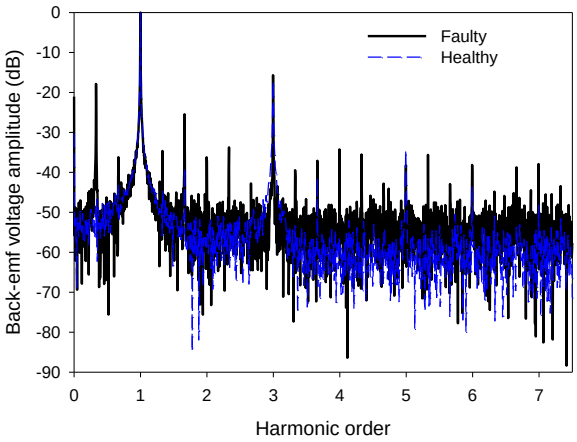

b)

Fig. 7. Experimental back-emf voltage induced in a pole of a phase winding (two slots) of a healthy and a faulty SPMSM operating as a generator. a) Normalized back-emf –with respect to the phase voltage– induced when operating at 6000 r/min. b) Back-emf voltage spectrum.

Fig. 8 shows the total back-emf induced in a phase of the stator windings of a healthy and a faulty SPMSM. Results from Fig. 8 show that in case of a faulty SPMSM, the back-emf amplitude is lower than for a healthy machine. It is worth noticing that the spectrum only contains odd harmonics which are due to the particular geometry of the machine. Therefore, the back-emf spectrum of the partially demagnetized SPMSM does not contain fractional harmonics. Thus, in summary, although the back-emf in a single pole of a phase winding contains fractional harmonics, they do not appear when considering an entire phase winding. This means that for the analyzed SPMSM, it is not feasible to diagnose this particular demagnetization by analyzing the fractional harmonics in the back-emf voltage or in the stator currents spectrum.

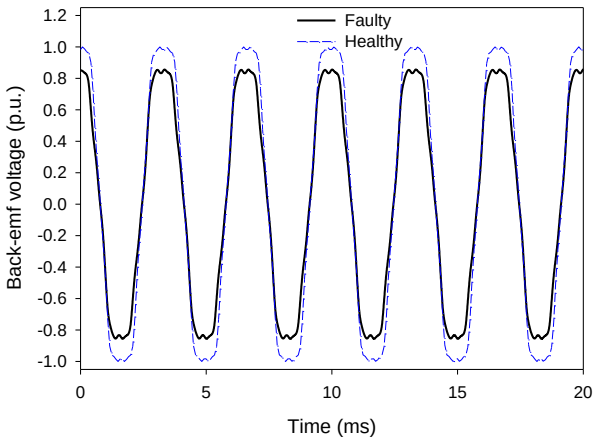

a)

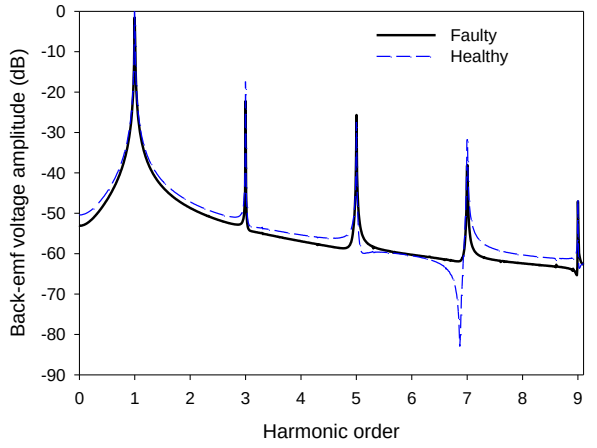

b)

Fig. 8. FEM simulations of healthy and a faulty SPMSM operating as a generator. a) Total back-emf induced in a phase winding (6 slots) when operating at 6000 r/min. b) Back-emf voltage spectrum.

The cancellation of the fractional harmonics in an entire series connected phase winding can be explained as follows. Every time a partially demagnetized pole passes in front of the first coil of phase *a* (coil a_1-$a_{1'}$ in Fig. 5), it induces a lower back-emf voltage amplitude compared with the ones induced in the other coils (a_2-a_2' and a_3-a_3'). The same analysis can be extended to coils a_2-a_2' and a_3-a_3'. The phase back-emf voltage in a series connected winding is the sum of all the coils voltages.

In order to illustrate this phenomenon a FEM simulation using the parameters in Table I has been carried out where the SPMSM was simulated with a full pole removed. These results are shown in Fig. 9, which proves that the entire back-emf induced in phase *a* has a lower amplitude (compared with a healthy machine) but it does not contain fractional harmonics.

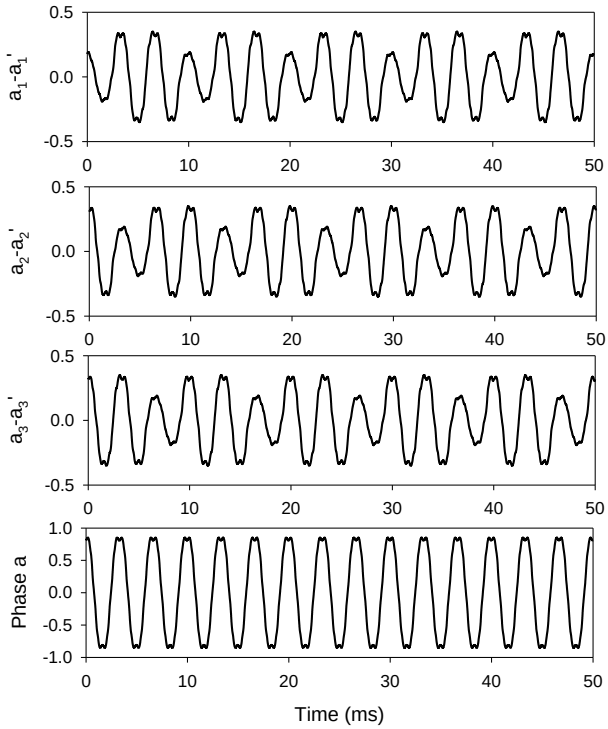

Fig. 9. Back-emf voltage –normalized with respect to the phase voltage– induced in a series connected winding obtained by means of FEM simulations supposing a full pole removed.

Fig. 10 proves that as in the case of the back-emf, when the machine operates as a motor, the stator currents only present odd harmonics due to the own geometry of the machine but they do not contain fractional harmonics. Hence, under the assumptions made in this work, the analysis of the current spectrum does not allow diagnosing these types of faults.

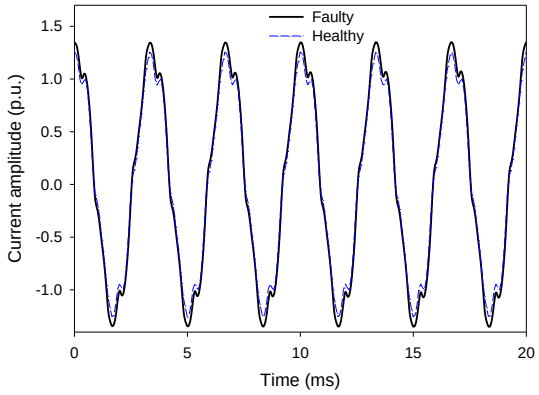

a)

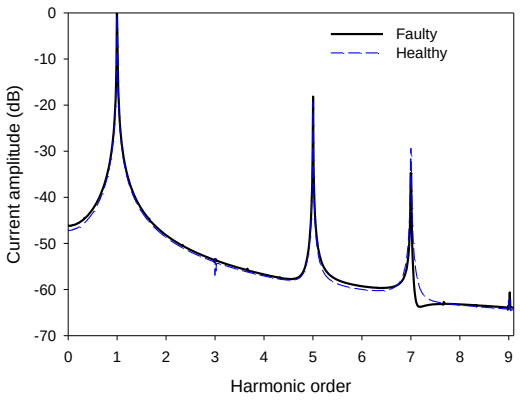

b)

Fig. 10. FEM simulations of the stator current of a healthy and a partially demagnetized SPMSM running at 6000 r/min under rated load. a) Current in phase *a* in p.u. normalized with respect to the rated current. b) Phase *a* current spectrum.

III. The Fault Severity Index

In order to carry out an online fault diagnosis scheme, it is highly desirable to use an easy-to-calculate fault severity index with low computational burden. This index allows quantifying the severity of a demagnetization fault.

The following assumptions are done. First, the rotor of a healthy SPMSM is supposed to have n identical magnets with the same remanence B_r. Second, it is assumed that the back-emf voltage in a phase winding e_{phase} is proportional to the number of magnets and also to the angular speed of the rotor. A partially demagnetized SPMSM may be understood as a machine with fewer completely magnetized magnets than a healthy one. Consequently a partially demagnetized SPMSM experiences a flux reduction and also a decrease in the back-emf voltage in a phase winding e_{phase}. This reduction ought to be proportional to the ratio between the number of effective magnets in the partially demagnetized machine over the total number of magnets in a healthy one. Consequently, the total back-emf in a phase winding may be written as

$$e_{faulty}(t)=\frac{n_{effective}}{n_{total}}\cdot e_{healthy}(t)=k\cdot e_{healthy}(t) \qquad (2)$$

where $e_{healthy}$ and e_{faulty} are, respectively, the phase back-emf in a healthy and a faulty machine, $n_{effective}$ is the number of effective or completely magnetized magnets in a faulty SPMSM and n_{total} is the number of rotor magnets in a healthy machine.

Factor k in (2) is the fault severity index proposed in this work, which allows quantifying the demagnetization degree of a given SPMSM. Thus, the factor k is easily obtained by comparing the back-emf with the reference back-emf when the machine was healthy.

As detailed in Fig. 1, the studied SPMSM has four removed magnets over a total of 24 (n_{total} = 24 and $n_{effective}$ = 20). Hence, the theoretical value of the factor k = 20/24 = 0.833, while FEM simulations lead to 0.832 which has been calculated by applying (2).

However, when the SPMSM acts as a motor the back-emf is not available. Therefore, another system to measure the factor k is required, as detailed in the next sections.

Additionally, the back-emf induced voltage matrix due to the permanent magnets can be written as

$$\frac{d}{dt}[\lambda_{PM,abc}]=\left[\frac{d\lambda_a}{dt}\ \frac{d\lambda_b}{dt}\ \frac{d\lambda_c}{dt}\right]^t \qquad (3)$$

IV. The ZSVC For Healthy And Partially Demagnetized SPMSMs

In this section the equation of the zero-sequence voltage component (ZSVC) is derived for both healthy and partially demagnetized machines.

In Section III it has been shown that when analyzing the proposed type of demagnetization no new harmonics appear in the stator currents spectrum of a faulty SPMSM. It is so because of the symmetrical configuration of the stator windings. However, analogous results may be obtained when dealing with other stator configurations [14]. Therefore, under these circumstances it is not feasible to analyze the stator currents spectrum. In these cases the ZSVC method allows detecting such faults. Note that the fundamental frequency of the ZSVC corresponds to the third harmonic of the back-emf spectrum.

Fig. 11 shows a diagram of the experimental setup proposed to measure the ZSVC. As SPMSMs are inverter fed machines, their stator windings usually have ZSVC injected by the inverter. Fortunately, by means of the inexpensive three-phase balanced resistor network shown in Fig. 11, the ZSVC generated by the inverter may be removed [15].

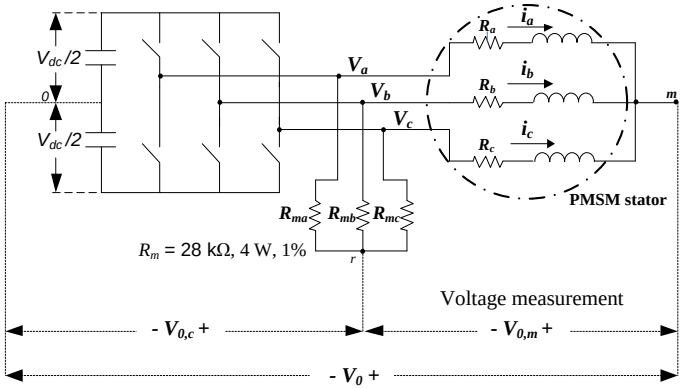

Fig. 11. Diagram of the SPMSM connection with the inverter, the stator windings and the resistor network used to generate an artificial neutral point.

The ZSVC method for fault diagnosis requires an accessible neutral point. For critical systems this disadvantage may be offset by the supplementary ability to detect incipient demagnetization faults. Additionally this system is compatible with fault tolerant schemes, since they usually need an accessible neutral point [11].

According to Fig. 11, the currents through the three balanced resistors must satisfy

$$i_{Rma}+i_{Rmb}+i_{Rmc}=0 \qquad (4)$$

where $R_{ma}=R_{mb}=R_{mc}=R_m$. Equation (4) leads to

$$\frac{V_a - V_{0,c}}{R_m} + \frac{V_b - V_{0,c}}{R_m} + \frac{V_c - V_{0,c}}{R_m} = 0 \quad (5)$$

From (5) it results

$$V_{0,c} = \frac{1}{3}(V_a + V_b + V_c) \quad (6)$$

where

$$V_0 = V_{0,c} + V_{0,m} \quad (7)$$

The balanced three-phase resistor network allows removing the ZSVC injected by the inverter from the neutral voltage of the machine. Consequently, the $V_{0,m}$ ZSVC is only influenced by the harmonics due to the particular geometry of the studied SPMSM [15]. Additionally, the online measurement of the $V_{0,m}$ voltage component allows scaling the voltage sensor according to the ZSVC magnitude, thus enhancing the sensitivity of the measuring system.

A) Equations of the SPMSM

Considering (2), the stator equations of a SPMSM in the *abc* reference frame can be expressed as [16],

$$[V_{s,abc}] = [R_{sh}]\cdot[i_{s,abc}] + [L_{sh}]\cdot\frac{d}{dt}[i_{s,abc}] + k\frac{d}{dt}[\lambda_{PM,abc}] + [V_0] \quad (8)$$

where the $[V_0] = V_0[1\ 1\ 1]^t$ term is due to the voltage difference between the center point of the stator windings and the neutral point of the three-phase voltage-source. This term is zero when neglecting the effects of the constructive harmonics. Additionally k is the fault severity index defined in Section III. Note that when dealing with a healthy machine, factor k theoretically should be 1. By adding the rows in (8) and taking into account (4) it results

$$V_0 = \frac{1}{3}(V_a + V_b + V_c) - k\frac{d\lambda_{PM,0}}{dt} \quad (9)$$

where $\frac{d\lambda_{PM,0}}{dt} = \frac{1}{3}\left(\frac{d\lambda_a}{dt} + \frac{d\lambda_b}{dt} + \frac{d\lambda_c}{dt}\right)$.

Substituting (7) into (9) for a partially demagnetized machine one obtains

$$V_{0,m} = -k\frac{d\lambda_{PM,0}}{dt} \quad (10)$$

In the case of a healthy machine, $k = 1$ and (10) results in

$$V_{0,m} = -\frac{d\lambda_{PM,0}}{dt} \quad (11)$$

From (10) and (11) the fault severity index proposed in this work to measure demagnetization faults may be obtained as in (12).

$$k = \frac{[V_{0,m}]_{faulty}}{[V_{0,m}]_{healthy}} \quad (12)$$

where the ratio shown in (12) is obtained from the fundamental harmonic amplitude of the $V_{0,m}$ ZSVC (third harmonic of the supply frequency).

V. Experimental Validation Of The ZSVC-Based Method

In order to validate the usefulness of the ZSVC-based method to diagnose demagnetization faults, a healthy and a partially demagnetized SPMSM were tested under different operating conditions. Fig. 12 shows the fundamental harmonic amplitude of the $V_{0,m}$ ZSVC (third harmonic of the supply frequency) for a healthy and partially demagnetized SPMSMs.

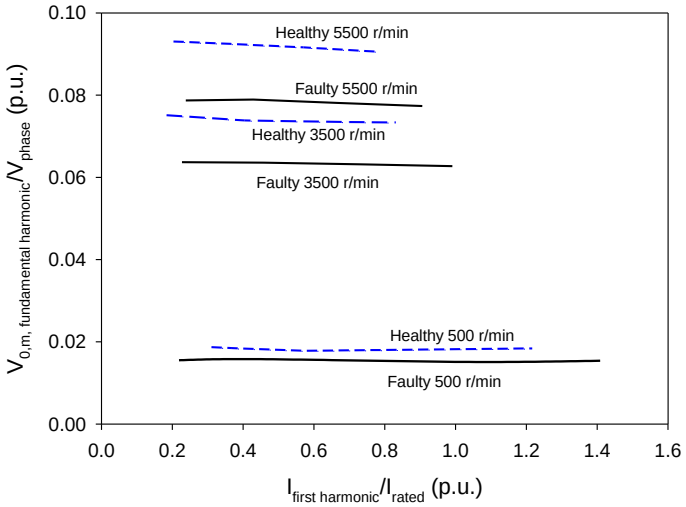

Fig. 12. Fundamental harmonic amplitude of the $V_{0,m}$ ZSVC plotted against the first harmonic amplitude of the current in a healthy and a faulty SPMSM when operating under different speeds and load conditions (different currents). Experimental results.

Results shown in Fig. 12 indicate that for a given speed, the amplitude of the fundamental harmonic of the $V_{0,m}$ ZSVC is almost constant regardless of the load level.

Fig. 13 plots the experimental relation between the fundamental harmonic amplitude of the $V_{0,m}$ ZSVC and the speed when operating under rated load.

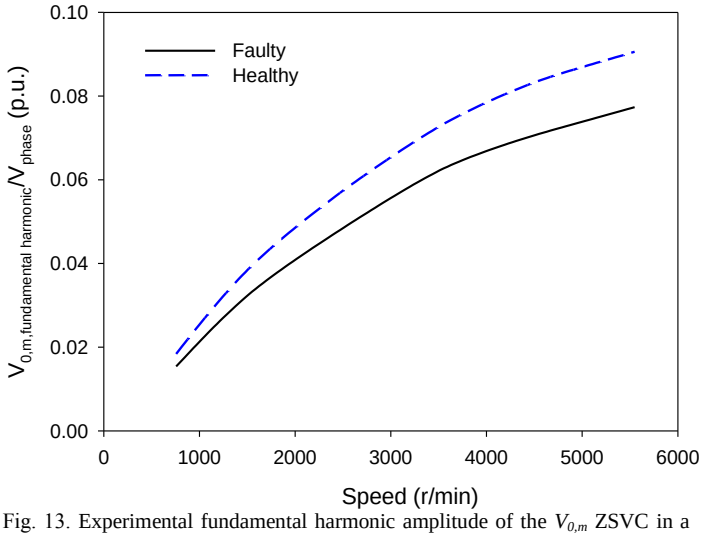

Fig. 13. Experimental fundamental harmonic amplitude of the $V_{0,m}$ ZSVC in a healthy and a faulty SPMSM when operating at different speeds under rated load.

Results shown in Fig. 13 indicate that for a given load level, the amplitude of the fundamental harmonic of the $V_{0,m}$ ZSVC increases with the speed. Note that it is not difficult to fit the response curve of the healthy machine by means of a 2nd order polynomial. Hence, the $V_{0,m}$ ZSVC of a practical machine may be compared with the value obtained by the adjusted polynomial, allowing obtaining the fault indicator presented in (12).

Table II summarizes the experimental results of the fault

severity index proposed in (12) when the partially demagnetized SPMSM operates at different speeds under rated load.

TABLE II
EXPERIMENTAL VALUE OF THE FAULT SEVERITY INDEX K WHEN THE SPMSM OPERATES UNDER RATED LOAD AND DIFFERENT SPEEDS.

Speed (r/min)	Fault indicator k in (12)
500	0.837
1500	0.841
2500	0.845
3500	0.855
4500	0.848
5500	0.854
Mean k	**0.847**
Theoretical k	**0.833**

Results from Table II validate the appropriateness of the fault indicator derived in this work.

From the results presented, the method proposed in this study works well for all types of windings except for those in which due to particular short pitching, the third harmonic of the back-emf is cancelled. Moreover, according to [14] when dealing with PMSMs with integral-slot symmetrical windings, no new harmonics due to demagnetization faults will appear in the current spectrum, thus making difficult to detect this type of faults by analyzing the current spectrum. Hence, the ZSVC method proposed in this work is more general than the current-based spectral method.

VI. CONCLUSIONS

Demagnetization faults may severely deteriorate SPMSMs performance, thus leading to a premature ageing or an irreversible fault condition. In this work a fault severity index to detect demagnetization faults in SPMSMs is proposed and evaluated by means of FEM simulations and experimental data. The proposed method is compatible with inverter fed machines and is particularly useful when dealing with fault tolerant systems. The proposed fault severity index can be obtained during normal operation of the machine, since with the accessible neutral point it is not necessary to stop the machine to measure the ZSVC and to perform the analysis. Features of the proposed method here include low computational burden, simplicity and high sensitivity. Additionally, simulated and experimental data prove that the value of the fault indicator provides reliable information about the severity of the fault. It has been shown that the convenience of the ZSVC-based methodology, because for the analyzed type of demagnetization the method based on the stator currents spectrum makes it difficult to detect demagnetization faults. The results presented in this work contribute to provide an efficient tool for identifying demagnetization faults in SPMSMs in its early stage. Hence, a corrective action (i.e. a scheduled stop or the activation of an alarm signal to limit the motor load among others) for guarantying a safe operation of the SPMSM may be implemented, thus avoiding a most severe fault of the machine.

VII. REFERENCES

[1] P. Zheng, J. Zhao, R. Liu, C. Tong, and Q. Wu, "Magnetic Characteristics Investigation of an Axial-Axial Flux Compound-Structure PMSM Used for HEVs," *IEEE Trans. Magn*., vol. 46, no. 6, pp. 2191–2194, Jun. 2010.

[2] J.R. Riba, J.A. Rosero, A. Garcia, and L. Romeral, "Detection of Demagnetization Faults in Permanent-Magnet Synchronous Motors Under Nonstationary Conditions," *IEEE Trans. Magn*., vol. 45 , no. 7, pp. 2961–2969, Jul. 2009.

[3] J.R. Riba, A. Garcia, and L. Romeral, "Demagnetization Diagnosis in Permanent Magnet Synchronous Motors under Non-Stationary Speed Conditions," *Electr. Pow. Syst. Res.*, vol. 80, no. 10, pp. 1277–1285, Oct. 2010.

[4] W. Le Roux, R. G. Harley, and T. G. Habetler, "Detecting rotor faults in permanent magnet synchronous machines," in *Proc. 4th IEEE Int. Symp. Diagnostics for Electric Machines, Power Electronics and Drives, SDEMPED*, 2003, pp. 198–203.

[5] W. Li, A. Li, and H. Wang, "Anisotropic fracture behavior of sintered rare-earth permanent magnets," *IEEE Trans. Magn*., vol. 41, no. 8, pp. 2339–2342, Aug. 2005.

[6] S. Yu and R. Tang, "Electromagnetic and mechanical characterization of noise and vibration in permanent magnet synchronous machines," *IEEE Trans. Magn.*, vol. 42, no. 4, pp. 1335–1338, Apr. 2006.

[7] K. C. Kim, S. B. Lim, D. H. Koo, and J. Lee, "The shape optimization of permanent magnet for permanent magnet synchronous motor considering partial demagnetization," *IEEE Trans. Magn*., vol. 42, no. 10, pp. 3485–3487, Oct. 2006.

[8] S. Ruoho, J. Kolehmainen, J. Ikaheimo, and A. Arkkio, "Interdependence of Demagnetization, Loading, and Temperature Rise in a Permanent-Magnet Synchronous Motor," *IEEE Trans. Magn*., vol. 46, no. 3, pp. 949–953, Mar. 2010.

[9] S. Rajagopalan, W. le Roux, T.G. Habetler, R.G. Harley, "Dynamic Eccentricity and Demagnetized Rotor Magnet Detection in Trapezoidal Flux (Brushless DC) Motors Operating Under Different Load Conditions," *IEEE Trans. on Power Electron*., vol. 22, no. 5, pp. 2061-2069, Sept. 2007.

[10] B. A. Welchko, T. A. Lipo, T. M. Jahns, and S. E. Schulz, "Fault tolerant three-phase AC motor drive topologies: a comparison of features, cost, and limitations," *IEEE Trans. Power Electr*., vol. 19, no. 4, pp. 1108-1116, Jul. 2004.

[11] O. Wallmark, L. Harnefors, and O. Carlson, "Control Algorithms for a Fault-Tolerant PMSM Drive," *IEEE Trans. Ind. Electron*., vol. 54, no. 4, pp. 1973-1980, Aug. 2007.

[12] J. C. Urresty, J. R. Riba, L. Romeral, and A. Garcia, "A Simple 2-D Finite-Element Geometry for Analyzing Surface-Mounted Synchronous Machines With Skewed Rotor Magnets," *IEEE Trans. Magn*., vol. 46, no. 11, pp. 3948-3954, Oct. 2010.

[13] W. le Roux, R. G. Harley, and T. G. Habetler, "Detecting Rotor Faults in Low Power Permanent Magnet Synchronous Machines," *IEEE Transactions Power Electron.* , vol. 22, no. 1, pp. 322-328, Jan. 2007.

[14] D. Casadei, F. Filippetti, C. Rossi, and A. Stefani, "Magnets faults characterization for Permanent Magnet Synchronous Motors," in *Proc. IEEE International Symposium on Diagnostics for Electric Machines, Power Electronics and Drives, SDEMPED 2009*, 2009, pp.1-6.

[15] F. Briz, M. W. Degner, P. Garcia, and A. B. Diez, "High-Frequency Carrier-Signal Voltage Selection for Stator Winding Fault Diagnosis in Inverter-Fed AC Machines," *IEEE Trans. Ind. Electron*., vol. 55, no. 12, pp. 4181-4190, Dec. 2008.

[16] L. Romeral, J. C. Urresty, J.R. Riba, and A. Garcia, "Modeling of Surface-Mounted Permanent Magnet Synchronous Motors With Stator Winding Inter-Turn Faults," *IEEE Trans. Ind. Electron*., vol. 58, no. 5, pp. 1576-1585, May 2011.